

End-to-End Reinforcement Learning of Curative Curtailment with Partial Measurement Availability

Hinrikus Wolf^{*†1}, Luis Böttcher^{*2}, Sarra Bouchkati^{*2}, Philipp Lutat²,
Jens Breitung¹, Bastian Jung³, Tina Möllemann³, Viktor Todosijević³,
Jan Schiefelbein-Lach⁴, Oliver Pohl⁵, Andreas Ulbig², and Martin Grohe^{†1}

¹ Computer Science, RWTH Aachen University
{hinrikus, grohe}@informatik.rwth-aachen.de

² IAEW, RWTH Aachen University
{l.boettcher, s.bouchkati, a.ulbig}@iaew.rwth-aachen.de

³ RWTH Aachen University

⁴ E.ON Group Innovation GmbH

⁵ Schleswig-Holstein Netz AG

Abstract—In the course of the energy transition, the expansion of generation and consumption will change, and many of these technologies, such as PV systems, electric cars and heat pumps, will influence the power flow, especially in the distribution grids. Scalable methods that can make decisions for each grid connection are needed to enable congestion-free grid operation in the distribution grids. This paper presents a novel end-to-end approach to resolving congestion in distribution grids with deep reinforcement learning. Our architecture learns to curtail power and set appropriate reactive power to determine a non-congested and, thus, feasible grid state. State-of-the-art methods such as the optimal power flow (OPF) demand high computational costs and detailed measurements of every bus in a grid. In contrast, the presented method enables decisions under sparse information with just some buses observable in the grid. Distribution grids are generally not yet fully digitized and observable, so this method can be used for decision-making on the majority of low-voltage grids. On a real low-voltage grid the approach resolves 100% of violations in the voltage band and 98.8% of asset overloads. The results show that decisions can also be made on real grids that guarantee sufficient quality for congestion-free grid operation.

Index Terms—Smart grids, Edge Computing, State Estimation, Optimal Power Flow, Deep Reinforcement Learning

I. INTRODUCTION

As part of the decarbonization of energy systems, new loads and generators are being connected to the distribution grids. The majority of electricity generation plants, such as photovoltaic and wind power plants, are being built decentrally. Furthermore, heat pumps and electromobility are replacing technologies that were previously based on fossil fuels. This changes and increases the power flow in the electricity grids, especially in the distribution grids.

This work was funded by E.ON SE in cooperation with E.ON Group Innovation GmbH, and Schleswig-Holstein Netz AG, who provided the grid topology.

^{*}These authors contributed equally to this work

[†]Funded by the European Union (ERC, SymSim, 101054974). Views and opinions expressed are, however those of the author(s) only and do not necessarily reflect those of the European Union or the European Research Council. Neither the European Union nor the granting authority can be held responsible for them.

To cope with this issue, customers' power demand or generation can be curtailed in cases of congestion. Independently of regulatory constraints, the need to decide which appliances connected to the grid must be curtailed to resolve the congestion exists. Solving an Optimal Power Flow (OPF) is the state-of-the-art approach to this question. However, to solve an OPF, measurements at every bus in the grid are needed. Often, such measurements are not available. A standard way of coping with missing measurements is to use state estimation techniques to predict the grid state on the basis of a few measurements and then apply optimal power flow to the predicted grid state. Current developments show that predicting grid states by using state estimation is a measure for distribution system operators to obtain complete information about their grid states. Unfortunately, state estimation is computationally expensive and introduces some inaccuracy.

Our approach, on the other hand, shows a novel method for obtaining curtailment decisions in power grids in an end-to-end fashion. Based on a few measurements, we utilize a model to predict curtailment decisions with high accuracy, which is deployable on low-cost edge computing devices. Our method uses the possibilities of reinforcement learning with partial observability by iteratively learning the curtailment decisions to obtain non-critical grid states. Reinforcement learning under partial observability finds normally application, e.g. in robotics [1], and video games [2].

A. Related work

Recent studies have demonstrated an increasing interest in utilizing Machine Learning (ML) techniques to estimate the solution of AC-OPF. This is achieved either by supervised learning, through self-supervised approaches or using Reinforcement Learning (RL) paradigms. Some of the early works relied on constrained supervised training. The work [3] incorporated the Karush-Kuhn-Tacker (KKT) conditions as penalty terms during training, while [4] combines a Multi-Layer Perceptron (MLP) with the Lagrangian Dual method. The effort in [5] leverages graph learning and implements a local and a global

Graph Neural Network (GNN) to solve the OPF problem. Although supervised approaches may yield promising results, they require the generation of pre-solved instances for training, which may be time-consuming and resource-intensive. Other approaches mitigate this drawback by relying on self-supervised training. A follow-up work to the method in [5] is presented in [6]. The key difference from the previous work is that the new method is trained using an unsupervised algorithm and a barrier method to satisfy the constraints. The work DC3 presented in [7] implements an MLP, where a completion step based on Newton’s Method is performed, and feasibility of the inequality constraints is ensured using a gradient-based correction step. On the other hand, other works exploit the self-learning ability of RL-agents and employ similar techniques for constrained learning to direct the RL agent in making physics-informed decisions. [8] and [9] rely on adding system specific Lagrangian parameters to the reward function, whereas the works in [10] and in [11] use the safety convex layer and holomorphic embedding based layer respectively to ensure feasibility.

A common thread among these approaches is the assumption of a fully observable grid state. However, in real-world scenarios, grids often lack full observability, with not all measurements from all grid participants readily accessible. This aspect presents an opportunity for developing a new method which takes reduced grid observability into consideration.

B. Main Contribution

This paper introduces a novel approach that leverages deep reinforcement learning to determine the level of curtailment for controllable buses, relying on a partially observable grid state. The method utilizes available grid measurements as inputs to a reinforcement learning agent, which directly determines the curtailment level for each bus. The agent undergoes training, following the typical reinforcement learning paradigm, within an environment that simulates the grid under the current supply task using power flow computations. To validate the proposed method, real low-voltage grid data from Schleswig-Holstein Netz AG and synthetic data representing realistic supply tasks are employed for training and validation. Results showcase the model’s efficacy in resolving nearly all instances of violations of physical constraints. Instances where violations persist are correctly identified by the model, however with insufficient curtailment

II. BACKGROUND

Optimal Power Flow (OPF) combines the economic dispatch of generation and load and the physical constraints through the power flow formulations. Optimal power flow is a nonlinear and non-convex, NP-complete, constrained optimization problem on power grids, commonly used in areas such as grid planning, power markets, and active grid operation and is a backbone in many calculations used to operate modern power systems [12], [13]. For that reason, there exist different types and modifications of the standard AC OPF problem, e.g., DC OPF, security-constrained OPF and others [14]. The

following formulation describes the Standard OPF problem. Let $\mathcal{G} = (\mathcal{V}, \mathcal{E})$ be a grid with buses \mathcal{V} and lines \mathcal{E} .

$$\min_y \sum_{i=0}^{|\mathcal{V}|-1} \sum_{k=0}^{n_c} c_{ik}(P_{g_i}^k) \quad (1a)$$

$$\text{subject to } S_{\text{bus}}(V_m, \Theta) - S(P_g, Q_g) = 0, \quad (1b)$$

$$P_g^{\min} \leq P_g \leq P_g^{\max}, \quad (1c)$$

$$Q_g^{\min} \leq Q_g \leq Q_g^{\max}, \quad (1d)$$

$$V_m^{\min} \leq V_m \leq V_m^{\max}, \quad (1e)$$

$$|S_f(V_m, \Theta)| \leq S^{\max}, \quad (1f)$$

$$|S_t(V_m, \Theta)| \leq S^{\max}, \quad (1g)$$

with $\Theta = \arg(V)$, $V_m = |V|$, $P_g = \text{Re}(S_g)$, and $Q_g = \text{Im}(S_g)$. Additionally, $c \in \mathbb{R}^{|\mathcal{V}| \times n_c}$, $n_c \in \mathbb{N}$ is the polynomial cost coefficient matrix; $S_{\text{bus}} \in \mathbb{C}^{|\mathcal{V}|}$ and $S_f, S_t \in \mathbb{C}^{|\mathcal{E}|}$ represent the complex bus and branch power injections. P_g^{\min} , P_g^{\max} , Q_g^{\min} , Q_g^{\max} , V_m^{\min} , $V_m^{\max} \in \mathbb{R}^{|\mathcal{V}|}$ and $S^{\max} \in \mathbb{R}^{|\mathcal{E}|}$ represent the different upper or lower constraints of the variables. OPF consists of three parts: equation 1a is the objective function of the minimization problem and represents the monetary cost of operating a power grid in the given state; equation 1b is the equality constraint of the problem, and represents the physical law of energy conservation; finally, equations (1c–1e) are the node-, and (1f–1g) edge-level inequality constraints, representing different technical limits of grid operation.

III. METHOD

The architecture needs a fixed grid topology with multiple supply tasks, which model different grid states including violations of lower or upper voltage bands, as well as line overloads. The architecture shall learn to resolve these violations by curtailing active and reactive power at certain buses with flexibility, which are explicitly listed as *controllable*. However, in reality, not all of the buses have measurement equipment installed. Therefore, the architecture only gets measurements of *observable* buses. We assume that every controllable bus is also observable. At the observable buses, measurements of P, Q and V are taken. Additionally, we supply valid ranges $[P_i^{\min}, P_i^{\max}]$ and $[Q_i^{\min}, Q_i^{\max}]$ for each controllable bus i . The architecture shall learn the optimal setpoint for P and Q at the controllable buses based on the restricted measurements (or observation).

A. Data Generation

To create datasets, it is necessary to map different grid operating states on which decisions have to be made. The dataset should encompass both non-critical and critical operational states to enable effective learning during training. By including a variety of scenarios, ranging from normal to critical states, the model can discern patterns and distinctions between the two. This ensures that the detection of critical states can be informed by the characteristics of non-critical states, facilitating a comprehensive learning of grid dynamics. The second aspect is the mapping of curtailment decisions in the grid so that flexible assets in the grid are curtailed in such a way that a

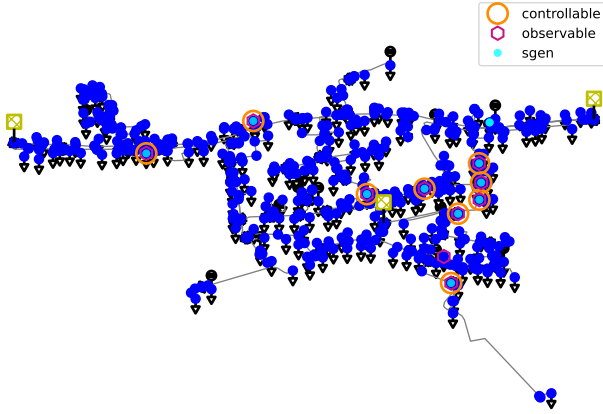


Fig. 1: Low Voltage grid with 7% observability (provided by Schleswig Holstein Netz GmbH)

non-critical grid state can be created from a critical grid state by the model’s decision.

Since, in many cases, grid models do not contain detailed information on the supply task, the first step is to assign an annual time series to the grid model. These are based on the technologies installed at the nodes, such as photovoltaics and household loads [15], [16]. The controllable installed technologies are assigned cost coefficients c (cf. Eq. 1a) so that their optimal use is incited. In addition, observable and non-observable nodes are defined in the grid, which should represent nodes in reality with measurement technology.

Based on the modelled supply task on the grid, both a power flow and an optimal power flow on the grid are calculated. When calculating the optimal power flow, the grid is assumed to be completely observable. For comparison, a state estimation is also calculated in combination with an optimal power flow in order to take account of the incomplete observability and to obtain a reference for the model to be trained here.

The calculation is carried out for at least 35.040 quarter-hour values in order to represent an annual simulation. In the course of development, it has been shown that further augmentation of the reference time series on the basis of the annual simulation is expedient, in particular, to increase the number of critical grid states in the dataset in order to achieve a higher accuracy of the trained model. An example grid is presented in Fig. 1.

The dataset, therefore, consists of tuples of unsolved and solved optimal power flow as well as an extension by a state estimation and optimal power flow on reduced observability.

B. Environment

The environment can be interpreted as a simulation of the physical world. It has a fixed grid topology, which gets updated with the corresponding supply task in every training step. The agent can interact with the environment by making an observation, i.e. collecting measurements at all observable buses. Based on this observation, the agent computes an action by choosing P and Q setpoints, which are applied to the grid. A power flow is computed with a Newton-Raphson procedure to simulate the effect of the agent’s decision. Based on the

overall resulting state of the environment (which includes measurements at buses not observable by the agent), a reward is given to the agent.

C. Reward

Let n be the number of buses, k the number of controllable generators and ℓ be the number of lines. Let \mathbf{V} be the vector of voltages of the buses in the current state, and denote by \mathbf{V}^{\min} and \mathbf{V}^{\max} the vector of lower and upper limits for the voltage band. We define the voltage loss $\mathcal{L}_V := \max_{i \in \{1, \dots, n\}} |\mathbf{V} - \text{clamp}(\mathbf{V}, \mathbf{V}^{\min}, \mathbf{V}^{\max})|_i$ as the maximum deviation from the voltage band. Formally, for vectors $\mathbf{x}, \mathbf{a}, \mathbf{b} \in \mathbb{R}^n$ we define $\text{clamp}(\mathbf{x}, \mathbf{a}, \mathbf{b}) := \max(\mathbf{a}, \min(\mathbf{x}, \mathbf{b}))$ where \min and \max are applied pointwise. Similarly, for the vector of relative loads \mathbf{I} we let $\mathcal{L}_I := \max_{i \in \{1, \dots, \ell\}} \max(\mathbf{I} - \mathbf{1}, \mathbf{0})_i$ be the maximum relative line load violation. Further, we define the curtailment cost as $\mathcal{C}_P := \frac{1}{|\mathcal{C}|} \sum_{i=1}^{|\mathcal{C}|} \mathbf{C}_i$ where \mathbf{C}_i is the amount of power curtailed at the i -th controllable generator. The agent obtains a reward of -10 if the power flow (computed after applying the agent’s actions) does not converge. Otherwise, the agent obtains

$$\mathcal{R} := \begin{cases} -\min\left(\frac{\mathcal{L}_V}{s} + \mathcal{L}_I, 1\right) & \text{if } \mathcal{L}_V + \mathcal{L}_I > 0, \\ 1 - \frac{\mathcal{C}_P}{s} & \text{otherwise,} \end{cases}$$

where $s := \frac{\lambda}{k} \cdot \sum_{i=1}^k |\mathbf{P}_i^{\max} - \mathbf{P}_i^{\min}|$ for a $\lambda > 1$. Since $\mathcal{C}_P \leq s$, we have $\mathcal{R} \in [-1, 1]$ if the Power Flow converges. Importantly, any action that results in no violations is strictly better than all actions that lead to violations. This is done to incentivize the agent to resolve critical grid states. However, this reward is not continuous due to the step of size s when moving from states with violations to those without. Note that the reward comprises information not available to the agent, specifically voltage and line load violations at buses that are not observable.

D. Architecture

The agent that determines the P and Q setpoints is a neural network obtained from an Actor-Critic model, which we train using Deep Deterministic Policy Gradient (DDPG) [17]. Both Actor and Critic are simple multi-layer perceptrons with two hidden layers, each of width 512.

We have implemented the model in PyTorch [18] with TorchRL [19]. For the environment, we re-implemented py-power’s [20] Newton-Raphson in PyTorch for more efficient computation, as we can compute the power flow on the GPU. This has two advantages, the power flow computes faster, second we avoid copying data between GPU and main memory which has a tremendous overhead.

E. Training Procedure

Reinforcement learning is often used when decisions from the past influence the future, e.g. balancing a pendulum facing upwards. In our setting, this is not clearly the case because the power flow in the grid can change heavily when a car is plugged into a charger, for example. So, from one time step to another, a decision that was made before could be totally wrong because customer behaviour resolved the congestion. Because

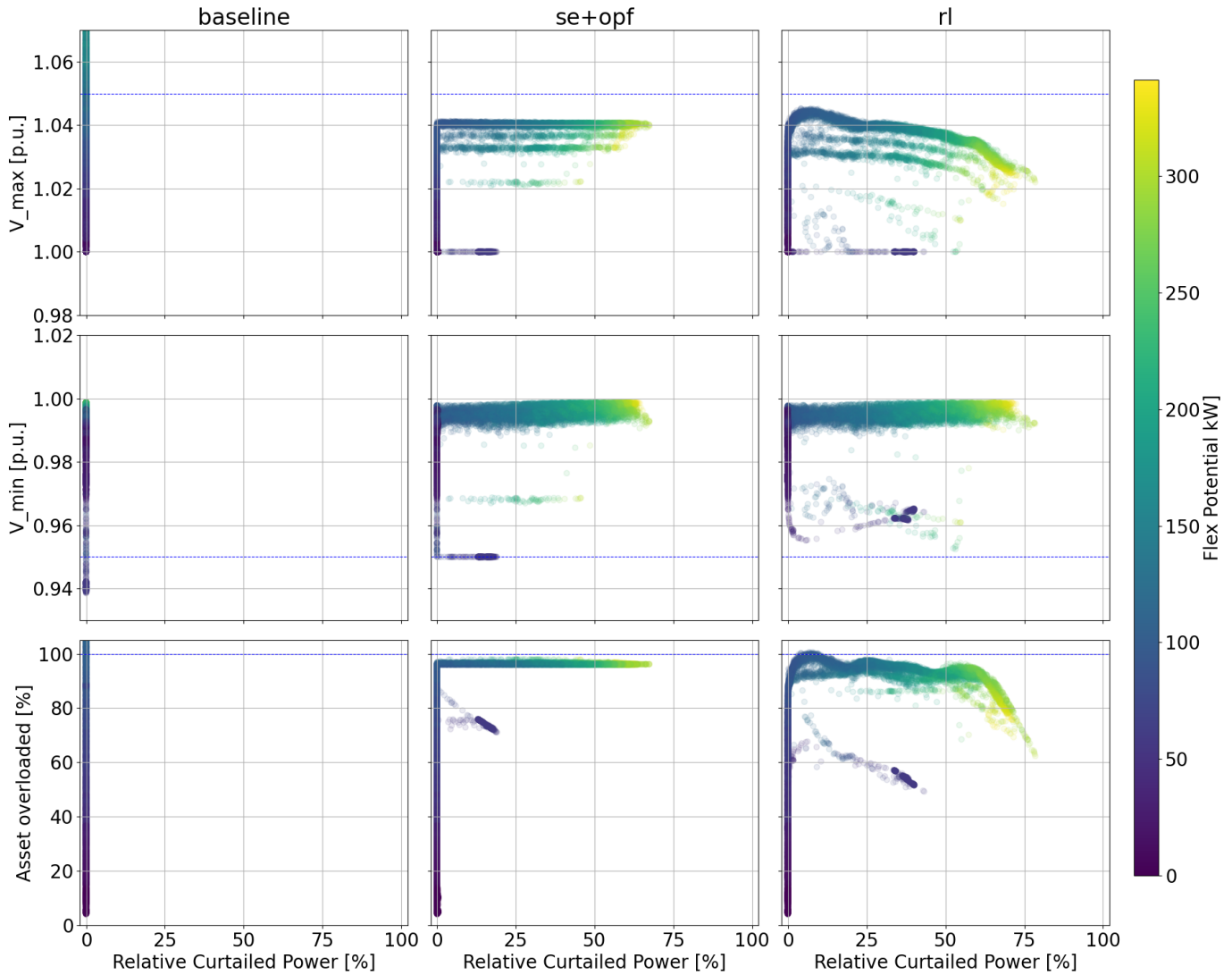


Fig. 2: Relative P Curtailment against the physical limits. Each point in each box corresponds to one supply task. In the column `baseline` is the case where every flexible bus is on its maximum set point, the columns `se+opf` and `rl` contain each the solutions of state estimation and OPF and our model. The colour of each point corresponds to the sum of the flexibility of all busses in that supply task.

of this, even though we are able to generate time-series data, the agent only sees the state at one timestep, and its actions depend on this one. For stability purposes, we hence shuffle the timesteps for training.

We train the agent’s policy based on experiences collected from the agent’s interactions with the environment. Since DDPG is an off-policy algorithm inherently deterministic, we add exploration noise (generated by an Ornstein-Uhlenbeck Process [21] with $\vartheta = 0.355$ and $\sigma = 0.6$) to the output of the Actor. Experiences are collected in a Replay Buffer of size 200,000 from which we sample 100 individual experiences uniformly at random at a time, which are then used to train the Actor and Critic networks.

IV. EXPERIMENTS

We conduct our experiments on a real low voltage grid of Schleswig-Holstein Netz AG (depicted in Figure 1), to which we apply our data generation method described in Section III-A. In cases where no flexibility is available on neither P nor Q at any bus, we dropped the supply task from the dataset since there is nothing to learn as $\mathbf{P}^{\min} = \mathbf{P}^{\max}$ and $\mathbf{Q}^{\min} = \mathbf{Q}^{\max}$. After this clean-up step, 20,453 supply tasks are still available. The distribution of violations is depicted in Table I.

To enlarge our training set, we performed data augmentation, where we added noise to the bounds for P^{\min} , P^{\max} . The set points of each augmented bus are set to its maximum. We augment cases with violation of the lower voltage band ten times in total to increase their representation. We kept the

TABLE I: Distribution of violations in test dataset (size: 20,453) and the ratio of resolved violations. Note that violations in either category are non-exclusive.

Violations	Number	Solved
Total	7,041	99.7%
Upper Voltage Band	5,384	100%
Lower Voltage Band	424	100%
Asset Overloaded	6,617	98.8%

unaugmented supply task as test data and trained only on the augmented data. We train on shuffled data in batches of each 20 supply tasks. The model gets each time-step five times in a row. Except for the first time, the set-points were adapted according to the model’s previous decision, so the model has the chance to correct previous decisions. We trained for 1,200,000 steps, so 240,000 different training samples (of augmented data), each five times. We run our experiments on a desktop computer with an AMD Ryzen 7 7700X processor and an NVIDIA GeForce RTX 4070 Ti GPU.

For our baselines, we take the state estimation from pandapower [22] together with the OPF solver from pypower [20] and the OPF with complete information. Since our state estimation is relatively exact, there are only minor differences between `se+opf` and the OPF alone. Thus, we only depict the results of `se+opf`.

In Figure 2 are depicted the test results of our model in comparison to `baseline` and `se+opf` (state estimation + OPF). In this case, we call `baseline` the case where every bus with flexibility is on its maximum set point. Each of the scatter plots contains all supply tasks. On the x axes, the *relative curtailment* of the current grid state is visualised. The relative curtailment is the ratio of the sum of absolute power output or input, respectively, at each controllable bus and the maximal flexibility. The colour of each point corresponds to maximal flexibility in kW. On the y axes, we plot the upper voltage band (top), the lower voltage band (middle), and the relative asset load (bottom), each with their corresponding limits (blue dashed line). In the `baseline` column, there is no curtailment visible, but several violations. In the `se+opf` column, there has been curtailment, which fixes all the violations. Starting in the upper voltage band, the limit is at 1.05p.u. All cases are below that line, even under 1.04p.u. In the plot of the lower voltage band, there are again no violations remaining, and the lowest points are all on the 0.95p.u. line. A similar behaviour can be seen in the plot for asset overload, where many points are now lying on the 100% line. Last, the reinforcement learning model shows a similar behaviour as `se+opf`. However, there is much more noise in the data. Except for 22 cases in the asset overload, all violations have been resolved by the RL agent. Though the RL agent detects these 22 cases as violations, it does not curtail them sufficiently. In a direct comparison of `se+opf` and the RL model, there are substantial similarities: in the upper voltage band, there are clusters of points in different lines, which are visible in both plots. In the lower voltage band, clusters of points appear in similar regions, although

TABLE II: Average Computation and Training Times

Training (total)	Inference (per supply task)	OPF	OPF+SE
8h	0.09s	0.31s	51s

with a more extensive spread. The same behaviour can be seen in the plot for asset overload. These clusters correspond to the different strands of the grid. The RL model shows much more noise on these “structures” and more curtailment. We also analysed our model’s output for Q , which is close to the output of `se+opf`.

V. DISCUSSION

The results show that the model behaves similarly to the OPF, probably owing to the design of the reward function, which penalises violations and encourages minimal curtailment, a feature shared with traditional OPF solvers. Nevertheless, the model still tends to curtail a higher amount of power compared to the OPF. In addition, a correlation between the amount of curtailment and the flexibility available in the system is observable. Test cases in which violations persist after the agent’s action indicate that the agent responds appropriately, but falls short of curtailing power sufficiently. This shortfall is observed for lower voltage band violations and may be due to their under representation in the training data. On the other hand, the model occasionally opts for curtailment even in the absence of detected violations, a behaviour observed in 25% more cases compared to the OPF. However, the magnitude of the curtailment in such cases remains minimal. Notably, in terms of computational efficiency, the model exhibits an inference time almost four times faster than the OPF and approximately 566 times faster than combined state estimation with the OPF. This significant acceleration renders the method highly attractive for real-time applications.

VI. CONCLUSION

We introduce a machine learning model for solving state estimation and OPF in end-to-end fashion. We train and validate our model on real grid data and show that the model is able to detect and counteract violations in most cases, while being faster than traditional solvers. Although the model does not provide a sufficient amount of curtailment in some cases, it correctly detects all violations. This drawback could be mitigated with more training data and further fine-tuning of the hyperparameters. For future work, the model could be extended to quantify the uncertainty of its output. In grid operation, the decisions of the models would only be applied if the model is certain of its decision. The overall accuracy could be improved by using ensembles of embeddings, where the outputs are ranked by their (un)certainly.

REFERENCES

- [1] W. Zhao, E. Rantala, J. Pajarinen, and J. P. Queralta, “Less is more: Robust robot learning via partially observable multi-agent reinforcement learning,” *CoRR*, vol. abs/2309.14792, 2023. [Online]. Available: <https://doi.org/10.48550/arXiv.2309.14792>

- [2] J. Gehring, D. Ju, V. Mella, D. Gant, N. Usunier, and G. Synnaeve, "High-level strategy selection under partial observability in starcraft: Brood war," *CoRR*, vol. abs/1811.08568, 2018. [Online]. Available: <http://arxiv.org/abs/1811.08568>
- [3] R. Nellikkath and S. Chatzivasileiadis, "Physics-informed neural networks for minimising worst-case violations in dc optimal power flow," in *2021 IEEE International Conference on Communications, Control, and Computing Technologies for Smart Grids (SmartGridComm)*. IEEE, 2021, pp. 419–424.
- [4] F. Fioretto, P. V. Hentenryck, T. W. K. Mak, C. Tran, F. Baldo, and M. Lombardi, "Lagrangian duality for constrained deep learning," pp. 118–135, 2020. [Online]. Available: https://doi.org/10.1007/978-3-030-67670-4_8
- [5] D. Owerko, F. Gama, and A. Ribeiro, "Optimal power flow using graph neural networks," pp. 5930–5934, 2020. [Online]. Available: <https://doi.org/10.1109/ICASSP40776.2020.9053140>
- [6] —, "Unsupervised optimal power flow using graph neural networks," 2022. [Online]. Available: <https://doi.org/10.48550/arXiv.2210.09277>
- [7] P. L. Donti, D. Rolnick, and J. Z. Kolter, "DC3: A learning method for optimization with hard constraints," 2021. [Online]. Available: <https://openreview.net/forum?id=V1ZHVxJ6dSS>
- [8] Z. Yan and Y. Xu, "Real-time optimal power flow: A lagrangian based deep reinforcement learning approach," *IEEE Transactions on Power Systems*, vol. PP, pp. 1–1, 04 2020.
- [9] T. Wu, A. Scaglione, and D. Arnold, "Constrained reinforcement learning for stochastic dynamic optimal power flow control," in *2023 IEEE Power & Energy Society General Meeting (PESGM)*. IEEE, 2023, pp. 1–5.
- [10] A. R. Sayed, C. Wang, H. I. Anis, and T. Bi, "Feasibility constrained online calculation for real-time optimal power flow: A convex constrained deep reinforcement learning approach," *IEEE Transactions on Power Systems*, vol. 38, no. 6, 2023.
- [11] A. R. Sayed, X. Zhang, G. Wang, C. Wang, and J. Qiu, "Optimal operable power flow: Sample-efficient holomorphic embedding-based reinforcement learning," *IEEE Transactions on Power Systems*, vol. 39, no. 1, pp. 1739–1751, 2024.
- [12] M. B. Cain, R. P. O'neill, A. Castillo *et al.*, "History of optimal power flow and formulations," *Federal Energy Regulatory Commission*, vol. 1, pp. 1–36, 2012.
- [13] D. Bienstock and A. Verma, "Strong NP-hardness of AC power flows feasibility," *Operations Research Letters*, vol. 47, no. 6, pp. 494–501, 2019.
- [14] S. Frank and S. Rebennack, "An introduction to optimal power flow: Theory, formulation, and examples," *IIE transactions*, vol. 48, no. 12, pp. 1172–1197, 2016.
- [15] C. M. Vertgevall, C. Hölscher, L. Böttcher, J. Bigalke, and A. Ulbig, "Modeling and application of probabilistic electrical household loads in distribution grid simulations," in *2022 International Conference on Smart Energy Systems and Technologies (SEST)*. IEEE, 2022, pp. 1–6.
- [16] S. Meinecke, D. Sarajlić, S. R. Drauz, A. Klettke, L.-P. Lauven, C. Rehtanz, A. Moser, and M. Braun, "Simbench—a benchmark dataset of electric power systems to compare innovative solutions based on power flow analysis," *Energies*, vol. 13, no. 12, p. 3290, 2020.
- [17] T. P. Lillicrap, J. J. Hunt, A. Pritzel, N. Heess, T. Erez, Y. Tassa, D. Silver, and D. Wierstra, "Continuous control with deep reinforcement learning," in *4th International Conference on Learning Representations, ICLR 2016, San Juan, Puerto Rico, May 2-4, 2016, Conference Track Proceedings*, Y. Bengio and Y. LeCun, Eds., 2016. [Online]. Available: <http://arxiv.org/abs/1509.02971>
- [18] A. Paszke, S. Gross, F. Massa, A. Lerer, J. Bradbury, G. Chanan, T. Killeen, Z. Lin, N. Gimelshein, L. Antiga, A. Desmaison, A. Kopf, E. Yang, Z. DeVito, M. Raison, A. Tejani, S. Chilamkurthy, B. Steiner, L. Fang, J. Bai, and S. Chintala, "Pytorch: An imperative style, high-performance deep learning library," in *Advances in Neural Information Processing Systems 32*, H. Wallach, H. Larochelle, A. Beygelzimer, F. d'Alché-Buc, E. Fox, and R. Garnett, Eds. Curran Associates, Inc., 2019, pp. 8024–8035. [Online]. Available: <http://papers.neurips.cc/paper/9015-pytorch-an-imperative-style-high-performance-deep-learning-library.pdf>
- [19] A. Bou, M. Bettini, S. Dittert, V. Kumar, S. Sodhani, X. Yang, G. D. Fabritiis, and V. Moens, "Torchrl: A data-driven decision-making library for pytorch," 2023.
- [20] R. D. Zimmerman, C. E. Murillo-Sánchez, and R. J. Thomas, "Matpower: Steady-state operations, planning, and analysis tools for power systems research and education," *IEEE Transactions on Power Systems*, vol. 26, no. 1, pp. 12–19, 2011.
- [21] G. E. Uhlenbeck and L. S. Ornstein, "On the theory of the brownian motion," *Phys. Rev.*, vol. 36, pp. 823–841, Sep 1930. [Online]. Available: <https://link.aps.org/doi/10.1103/PhysRev.36.823>
- [22] L. Thurner, A. Scheidler, F. Schafer, J. H. Menke, J. Dollichon, F. Meier, S. Meinecke, and M. Braun, "pandapower - an open source python tool for convenient modeling, analysis and optimization of electric power systems," *IEEE Transactions on Power Systems*, 2018. [Online]. Available: <https://arxiv.org/abs/1709.06743>